

PHOTOPHYSICAL PROPERTIES OF QUINOLINOID ANTIMALARIAL DRUGS AND THEIR EVALUATION AS HUMAN SERUM ALBUMIN ESTERASE INHIBITORS

David E. Couch, Lauren A. Blackwelder*, David M. Calvo*, Cosmo D. Cao*, Hannah G. Castellan*, Christian M. Cosner*, Lynsey K. Geray*, Emily R. Hofmann*, Kyle D. Kramer*, Garrett D. Kuchan*, Mikhail B. Lachapelle*, Kristi C. Lee*, Madelyn L. Letendre*, Tiffany H. Li*, Johnnay A. Martin*, Robert Martinez*, Evelyn M. McBride*, Isabella A. Mullally*, Joshua B. Quarterman*, Isabella R. Ratzlaff*, Mikhail A. Stiffler*, Nicholas W. Surina*, Thomas B. Swalm*, Katelyn D. Thompson*, Abigail E. Worley*, Eileen Zhao* and Barry W. Hicks†

United States Air Force Academy, Department of Chemistry, United States Air Force Academy, CO 80840

Abstract

The photophysical properties and human serum albumin (HSA) anti-esterase activities of ten compounds containing the quinoline functional group present in quinine and related antimalarial analogs were studied. Two different substrates with different acyl chains, para-nitrophenyl acetate (PNPac) or para-nitrophenyl myristate (PNPMy) were used for esterase kinetic studies. Using PNPac, HSA esterase activity did not follow Michaelis-Menten kinetics, nor was the enzymatic activity appreciably inhibited by quinolinoids, even at concentrations approaching 1 mM. In contrast, using PNPMy, HSA did follow Michaelis-Menten kinetics, and the enzymatic activity was decreased by quinolinoids with IC_{50} values near 300 μ M. However, the effective concentrations of quinolinoids against HSA were roughly 100-fold higher than those required to inhibit the esterase activity of butyrylcholinesterase. SwissDock studies suggest that while quinolinoids are competitive inhibitors with respect to butyrylcholinesterase, they bind away from the hypothesized catalytic site of HSA. Thus, antimalarial quinolinoids are not effective broad-spectrum anti-esterase inhibitors.

†Corresponding author: barry.hicks@afacademy.af.edu

* Undergraduate researchers and co-authors

Keywords: Human Serum Albumin, Esterase activity, Antimalarial Drugs

Received: May 23, 2024

Accepted: May 26, 2024

Published: June 13, 2024

Introduction

Approximately 60 percent of blood's protein content is human serum albumin (HSA); it is the most abundant globular protein found in human blood and plasma (1). HSA primarily serves as a transport protein for fatty acids and hormones (2), but it is also vital for maintaining osmotic pressure and directing the pharmacokinetics of xenobiotics, including all prescription drugs (3). In addition to these principal functions, HSA has been discovered to moonlight as an enzyme that hydrolyzes esters, amides, and organophosphorus compounds (3,4). The esterase activity of HSA has been reported with drugs such as aspirin, sulbenicillin, salicylic acid, and nicotinate esters, and enzymatic activity can be monitored with esters of 4-nitrophenol (5).

Quinine and its analogues (quinolinoids) are drugs commonly used to treat malaria. In our previous research, quinolinoids were found to inhibit the esterase activity of butyrylcholinesterase (6). A large body of work also shows that many of these quinolinoids, like most pharmaceuticals, bind to albumin (7-14). Here we inves-

tigated whether these compounds are also broad-spectrum esterase inhibitors by examining their ability to inhibit the esterase activity of HSA.

Experimental Methods

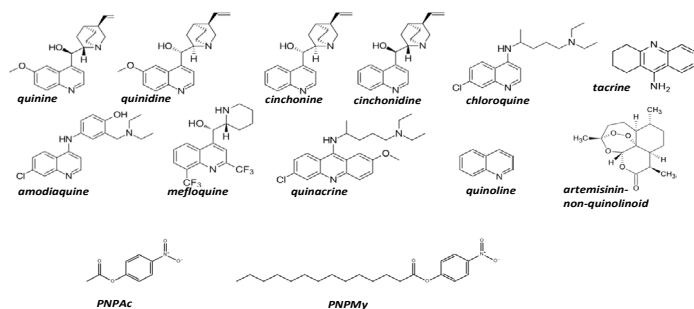
Materials

The quinolinoids and substrates used in this study are shown in scheme 1. Human serum albumin (HSA), 4-Nitrophenol (PNP), quinine, quinidine, chloroquine, tacrine, amodiaquine, mefloquine, quinacrine, and quinoline were purchased from Sigma-Aldrich (St Louis, MO), cinchonidine and cinchonine were purchased from TCI (Portland, OR). PNP was purchased from Alfa Aesar (Ward Hill, MA), PNPac was from Thermo Fisher Scientific (Waltham, MA), PNPMy (PNPMY) was from Biosynth (Staad, Switzerland), and artemisinin from Amazon (Seattle, WA). Artemisinin was extracted from 450 g of wormwood powder with 100 mL EtOH and was investigated as a control antimalarial lacking the quinoline functional group. Subsequently, the contents of the extraction process yielded a final stock solution with a concentration of 8 mM, as determined by spectrophotometry.

Photophysical Properties

Absorbance, excitation, and emission spectra (for the quinolinoids that had demonstrable emission) were obtained to define the parameters that could be used for quantum yield determinations. Quantum yields were determined by direct comparison of the analogs to quinine using 0.60 as the quantum yield for quinine in perchloric acid (15).

A stock solution was prepared for quinine and other quinolinoids within the concentration range of 0.1 to 10 mM depending



Scheme 1. The structures of the antimalarials and esterase substrates used in this work.

upon solubility in 0.1 M perchloric acid. To assess absorption, emission, and excitation maxima and quantum yields, standards from 10 to 100 μM were prepared in 0.1 M perchloric acid. The absorbance and fluorescence spectra for quinine and the other quinolinoids was determined using a Biotek Synergy 2 spectrofluorometer. Fluorescence lifetime analysis was conducted using an Edinburgh FLS1000 lifetimes fluorometer with excitation using either an NKT Photonics supercontinuum laser at 420 nm or diode lasers with wavelengths of 270 or 375 nm, all with TPSPC detection. Lifetimes were fit to single exponentials when data permitted, and two exponentials when it did not, based upon χ^2 values.

Enzyme Assays

All enzyme assays were conducted in a 0.1 Tris buffer containing 2 mM MgCl_2 , adjusted to pH 8, at 25° C. Stock solutions of were prepared at 10.0 mM for each of the quinolinoids in 5.0 mM HCl containing 2% DMSO. A standard curve was made with PNP concentrations from 0 to 50 μM . The curve was used to determine the molar extinction coefficient in our buffer so that changes in absorbance values could be converted concentration units from the kinetic activity data. PNP substrate stock solutions of 10 mM were prepared in EtOH.

HSA esterase activity was monitored at HSA concentrations of 2-10 $\mu\text{g/mL}$. Enzyme activity was measured with concentrations of PNPac substrates from 0 mM to 1000 μM or PNPMY at 0 to 200 mM. In all cases, DMSO never exceeded 5% and EtOH never exceeded 2% (v/v). Enzyme kinetics were monitored by visible spectroscopy at 400 nm using an Agilent BioTek Epoch Microplate Spectrophotometer with Gen2 software. Each solution was measured in triplicate in 96-well plates and enzyme activity was monitored at 400 nm for 2-10 min in 5 s intervals. Quinolinoid inhibition of HSA esterase was measured using quinolinoid solutions ranging from 4 nM to 1000 μM . HSA was equilibrated with the quinolinoid prior to data collection (~10 min).

In Silico Analysis

Docking studies of the affinity of HSA for each quinolinoid were performed using SwissDock (16). SwissDock is based upon EADock DSS, which samples the entire protein surface for binding grooves and estimates CHARMM energies within grids. Two structures from the Protein Data Bank (PDB), PDB IDs 7FFR and 1A06, were used to obtain the Gibb's Free Energy of binding of quinolinoids in various binding sites.

Results

Summary of Photophysical Properties

We found that the structure of the acyl chain portion of the substrate used for esterase activity can be a determinant in whether or not HSA esterase activity is observed (see below). It is also possible that the chromophore esterified to the acyl chain may also play a role, and we plan to examine that in future work. One alternative to monitoring absorbance changes of PNP esters by absorbance is to monitor umbelliferone esters hydrolysis by fluorescence spectroscopy, since several umbelliferone ester substrates are commercially available. Like quinine, umbelliferone (quantum yield 0.80-0.90) emits in the blue and the emission spectra substantially overlaps with that of quinine. To assess whether inhibition of HSA esterase activity by non-fluorescent quinolinoid

analog might also be possible using umbelliferone esters, the photophysical properties of all the analogs were examined. First absorbance and emission spectra were obtained from concentrated samples. Using quinine as a standard, the quantum yields were determined for all quinolinoids as shown for cinchonidine (Figure 1). No fluorescence at all was measured for amodiaquine. The fluorescence lifetimes of all the analogs with quantum yield at least 0.02 were also measured (Figure 2). Surprisingly, the range in values is more than an order of magnitude with quinacrine showing the shortest lifetime of 0.97 ns and quinoline showing the longest at 22 ns. Given the low values of the quantum yields for chloroquine, cinchonidine, cinchonine, quinoline, neutral red, and primaquine

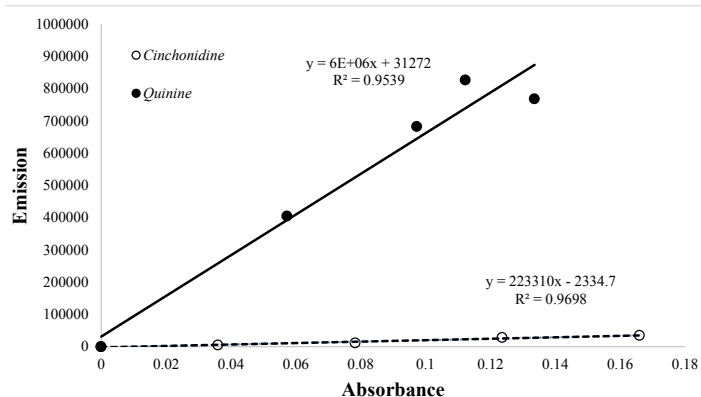


Fig. 1. Representative determination of quantum yield; in this example for cinchonidine ($\phi = 0.074$), relative to the quinine standard ($\phi = 0.60$). Of the 10 quinolinoids tested, quinine, quinacrine, tacrine and quinidine all showed significant fluorescent emission near 450 nm and cannot be tested in a fluorescence umbelliferone esterase assay. Exact quantum yield values for several quinolinoids were too small to accurately determine and are reported as <0.01 (see Table 1).

Table 1. Summary of the photophysical properties of quinolinoids.

	λ Abs max (nm)	ϵ ($\text{M}^{-1}\text{cm}^{-1}$)	λ Ex max (nm)	λ Em max (nm)	ϕ	τ (ns)
Quinine	349	5700	350	450	0.600	18.9
Chloroquine	342	18600	320	364	<0.01	-
Cinchonine	316	6830	314	420	0.017	-
Cinchonidine	316	10120	310	364	0.074	1.56
Quinacrine	425	8600	450	494	0.560	0.97, 3.31
Tacrine	320	1000	326	354	0.100	1.15
Quinoline	310	36121	350	440	0.039	22
Neutral Red	530	16500	526	680	<0.01	-
Primaquine	280	13700	328	365	0.019	-
Quinidine	350	2508	350	450	0.670	21.7

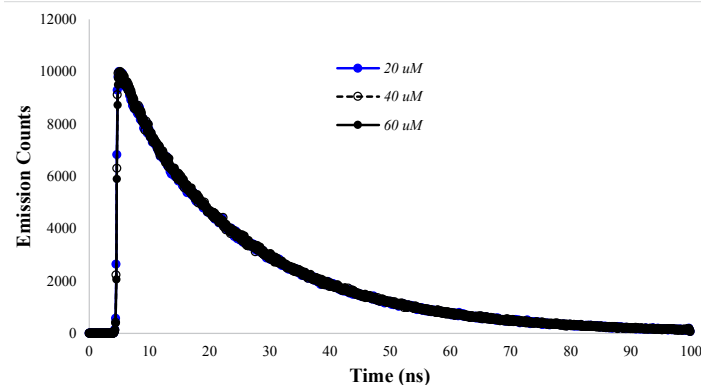


Fig. 2. Representative result from fluorescence lifetime determination; in this case for quinidine. The lifetimes were identical at three different concentrations. Like quinidine, most of the quinolinoids, except quinacrine, were well fit with single exponential decays.

these compounds might all be amenable to study by fluorescence using umbelliferone esters. However, quinine, quinacrine, tacrine and quinidine should not be assessed using umbelliferone esters as their emission would complicate data analysis.

PNP Spectrum and Standard Curve

The UV-Vis absorbance of PNP was evaluated over a range of wavelengths (350-500 nm) (Figure 3A) to convert spectrophotometric data to concentrations for kinetic analysis. The wavelength for maximum absorbance of PNP within this range was found to be 400 nm, and the molar extinction coefficient was determined to be $19900 \text{ M}^{-1}\text{cm}^{-1}$ in Tris buffer pH 8.0 containing 2 mM MgCl_2 (Figure 3B), which is close to previously published values (17). Standards of increasing PNP substrate concentration (0-50 μM) were analyzed with at 400 nm, demonstrating a linear relationship between absorbance and concentration.

Michaelis-Menten Initial Velocity Kinetic Analysis

In Figure 4A, the substrate was PNPMY and the esterase enzyme follows Michaelis-Menten kinetics and data was reformatted into a Lineweaver-Burke plot (inset). The K_m (116 μM) and V_{max} (0.030 $\mu\text{M/s}$) values were determined from the Lineweaver-Burke plot. These values resulted in a calculated k_{cat} value of 0.26 s^{-1} for PNPMY. In Figure 4B the HSA esterase activity versus substrate concentration showed a linear relationship, and thus, did not obey Michaelis-Menten kinetics. Values above 1000 μM could not be assayed due to the limited solubility of the long hydrophobic acyl

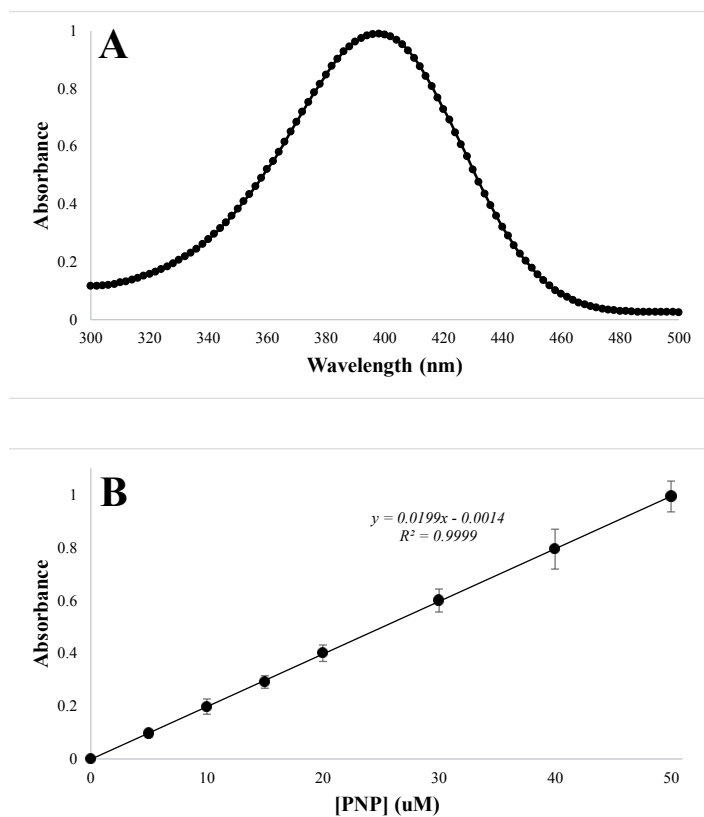


Fig. 3. Spectroscopic analysis of PNP. A. Absorbance spectrum of PNP (50 μM) solution in Tris buffer pH 8.0. The wavelength of maximum PNP absorbance was determined to be 398 nm. B. Standard curve of PNP absorbance at 398 nm versus PNP concentration (0-50 μM) with standard error bars amplified by two. All data was obtained with an Agilent BioTek Epoch Microplate Spectrophotometer. A strong, positive linear relationship was observed between absorbance and concentration of PNP.

chain. Using PNPAC much higher substrate concentrations could be analyzed, and the rate of PNP production was much higher at those concentrations, but the enzyme was not saturated under the conditions examined which are dictated by solubility limits.

IC_{50} Values of Quinine Inhibitors

Initial esterase reaction rates in the presence of varied inhibitor concentrations (30 nM - 1 mM) were evaluated. IC_{50} curves for quantitative comparison of inhibitor strength were generated for inhibitors in both PNPAC (Figure 5A) and PNPMY (Figure 5B). Although there is quite a range of scatter in the data, it clearly shows that none of the quinolinoids, with the possible exception of amodiaquine at very high concentrations, are capable of inhibiting the HSA esterase activity using PNPAC. However, with the exception of tacrine, all of the quinolinoids tested against HSA esterase using PNPMY demonstrated some ability to inhibit the enzymatic activity, albeit with a mean IC_{50} exceeding 300 μM . The most potent inhibitors were neutral red and artemisinin, neither of which is an antimalarial drug, and artemisinin is also not a quinolinoid.

In Silico Docking of Antimalarials to Human Serum Albumin

The binding energies between HSA and each antimalarial were determined using SwissDock. Two HSA structures from the PDB were used, PDB IDs 7FFR (Fig. 6A) and 1AO6 (Fig. 6B). The major domains and known drug binding sites, along with two potentially important residues locations are shown in Figure 6A.

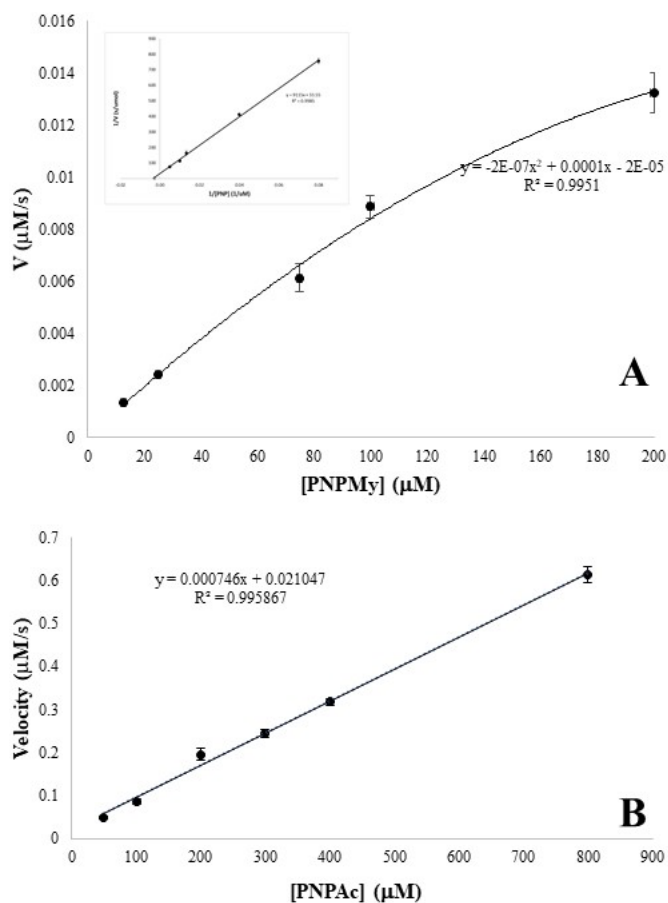


Fig. 4. Michaelis-Menten kinetic analysis of HSA with PNPMY and PNPAC. A. HSA obeys MM kinetics with PNPMY with a K_m value of 116 μM . B. Using PNPAC, a simple linear relationship is observed between the rate of substrate hydrolysis and concentration; that is, this substrate does not obey Michaelis-Menten kinetics as it fails to saturate the enzyme even at very high concentrations.

Most compounds tested had similar Gibbs Free Energy changes of approximately -7 to -8 kcal/mol upon binding with proteins. Examples of the protein-ligand complexes obtained are shown in Figure 6A for primaquine and Figure 6B for tacrine (inside dashed

circles). The complete ΔG values (most negative only for each compound) for each antimalarial are listed in Table 2. Although the two HSA proteins showed similar values for each ligand, many showed slightly tighter binding with 7FFR. All of the tightest quinolinoid binding sites were in 3 general locations as indicated in Fig 6B as white arrows.

Discussion

We have shown here that differences between the acyl chain of the ester substrates play a significant role in the ability to detect true HSA esterase enzymatic activity and its inhibition. When PNPac substrate was used, the esterase did not obey MM kinetics, and the enzyme was essentially uninhibited by quinolinoids. However, when using PNPMY, HSA does obey MM kinetics and it was demonstrated that some of the quinolinoid were capable of inhibiting the esterase activity. This agrees with previous findings and helps clarify a gap in the literature. Complete human serum contains many enzymes with esterase activity, and HSA was first shown to possess esterase activity by Wilde, et al, in 1964 (18). This esterase activity has been reaffirmed as recently as 2023 (19). There is a complex relationship between HSA esterase activity and a variety of drugs for reasons that remain uncertain (20). However, it has also been noted that some esterase substrates, including PNPac, are non-specific acylating agents which can act on as many as 82 amino acid sidechains of HSA (21), and this gives HSA a “pseudo-esterase activity”. Our work suggests that HSA may bind to longer chain acyl esters with greater selectivity than the smaller, more water soluble PNPac and be useful for examin-

Table 2. Ligand-Protein Complex Gibbs Free Energies

Ligand	Protein	ΔG (kcal/mol)
Amodiaquine	1ao6	-8.30
	7ffr	-7.79
Artemisinin	1ao6	-6.97
	7ffr	-7.32
Chloroquine	1ao6	-7.80
	7ffr	-8.26
Cinchonine	1ao6	-9.12
	7ffr	-8.09
Mefloquine	1ao6	-9.17
	7ffr	-7.97
Neutral Red	1ao6	-6.76
	7ffr	-7.18
Primaquine	1ao6	-7.15
	7ffr	-7.73
Quinacrine	1ao6	-7.86
	7ffr	-8.22
Quinidine	1ao6	-7.96
	7ffr	-8.20
Quinine	1ao6	-7.78
	7ffr	-7.85
Tacrine	1ao6	-8.24
	7ffr	-6.80

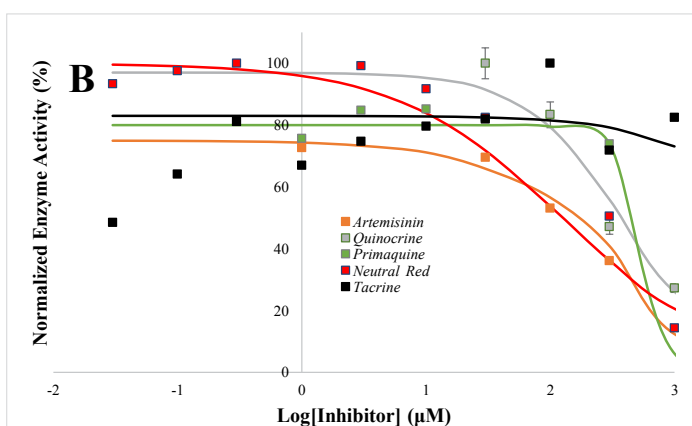
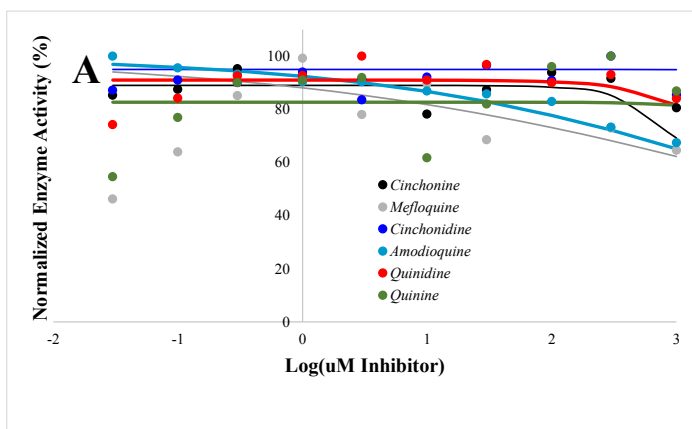


Fig 5. IC_{50} curves of quinolinoid inhibitors of HSA using either PNPac or PNPMY. In each case data were fit and optimized to sigmoidal curves in Excel. A. Using PNPac, there is little observable inhibition even at quinolinoid concentrations approaching 1 mM. It appears as though there may even be some stimulation of activity at lower concentrations. B. In contrast, using PNPMY, there was noteworthy inhibition from all quinolinoids as well as artemisinin. The mean IC_{50} values are in the 300 μ M range, with tacrine being the most effective inhibitor with an IC_{50} value of about 50 μ M.



Figure 6. SwissDock Ligand-Protein Complexes. A. This shows the major domains (I-III) and the known drug binding sites (called Sudlow site I and site II). The location of the putative catalytic Lys199 residue location is shown by the yellow arrow using PDB ID 7FFR, along with the most active residue towards acylation, Tyr411, using the green arrow. Primaquine is shown bound above site I on domain I within the white oval. B. Here chloroquine, inside white oval, is bound to PDB ID 1AO6. Most of the higher affinity quinolinoid binding sites are at one of three locations (white arrows), none of which are immediately adjacent to Lys199 or Tyr411, nor directly within the well-known Sudlow sites I & II.

ing true esterase inhibition. Examination of other substrates, including esters with other chromophores is warranted.

Conclusion

Our findings also suggest that the quinolinoid drugs are not broad-spectrum esterase inhibitors. Most of the antimalarial quinolinoid drugs have a positive charge at physiological pH due to a tertiary amine group in the side chain. Thus, it is perhaps not surprising that they have a relatively high affinity for butyrylcholinesterase, as they likely bind to competitively with respect to the enzymes' positively charged substrates, acetylcholine or butyrylcholine (6). However, HSA binding sites for both fatty acids and most drugs are on relatively hydrophobic portions of the protein surface, and these would be much less likely to bind to cationic drugs.

Acknowledgements

We would like to thank the Department of Chemistry at the US Air Force Academy and the Air Force Office of Scientific Research (AFOSR) through the Chemistry Research Center for funding this work.

References

1. Phuangasawai, O.; Hannongbua S.; Gleeson P. M. *J. Phys. Chem. B*, 2014, 118.41, 11886-11894.
2. Merlot A. M.; Kalinowski D. S.; Richardson D. R. *Front. Physiol.*, 2014, 5.
3. Gerasimova Y. V.; Knorre D. D.; Shakirov M. M.; Godovikova T. S. *Bio. & Med. Chem. Let.*, 2008, 18.20, 5396-5398.
4. Simone, G. D.; Maso A. D.; Ascenzi P. *Int J Mol Sci*, 2021, 10086.
5. Tatsumi A.; Okada M.; Inagaki Y.; Inoue S.; Hamaguchi T.; Iwakawa S. *Bio. Pharm. Bull.*, 2016, 39.8, 1364-1369.
6. Alali O. S.; Arbanas E. E.; Auleciems Z. J.; Becerra M.; Bishop A. A.; Carswell B. J.; et al. *J. Undergrad. Chem. Res.*, 2023, 22.1, 1-5.
7. Wanwimolruk, S. and Denton, J.R. *J. of Pharmacy & Pharmacology*, 1992, 44.10, 806-811.
8. Conn, H. L. & Luchi, R.J. *J. of Clin. Invest.*, 1961, 40.3, 509-516.
9. Zhang, T. & Li, D. *Spectrochimica Acta Part A: Molec. & Biomolec. Spectroscopy*, 2013, 112, 15-20.
10. Biçer, E. & Özdemir, N. *Russian J. of Electrochem.*, 2014, 50, 587-593.
11. Marković, O.S., et al. *Spectrochimica Acta Part A: Molec. & Biomolec. Spectroscopy*, 2018, 192, 128-139.
12. Saravanan, K., et al., *Spectrochimica Acta Part A: Molec. & Biomolec. Spectroscopy*, 2021, 259, 119856.
13. Samari, Fayeze, et al. *Eur. J. Med. Chem*, 2012, 54, 255-263.
14. Musa, K.A., et al. *Biopolymers*, 2020, 111.2, e23337.
15. Namara, K. & Waluk, J. *Anal. Chem.*, 2019, 91, 5389-5394.
16. Grosdidier, A., Zoete, V. & Michielin, O. *Nucleic Acids Res.*, 2011, 39 sup 2, W270-W277.
17. Hethey, J. A. M. E. S., et al. *J. Exp. Microbio. & Immun.*, 2002, 2, 33-38.
18. Wilde, C. E. & Kekwick, R.G.O. *Biochem. J.*, 1964, 91.2, 297.
19. Xia, H., et al. *RSC Advances*, 2023, 13.12, 8281-8290.

20. Tatsumi, A., et al. *Biological & Pharm. Bul.*, 2016, 39.8, 1364-1369.

21. Lockridge, O., et al. *J. Bio. Chem.*, 2008, 283.33, 22582-22590.